J Therm Anal Calorim (2010) 100:685–693
DOI 10.1007/s10973-009-0206-1

Theoretical prediction and experimental determination of room-temperature phase change materials using hydrated salts as agents

Bihai Li · Dewen Zeng · Xia Yin · Qiyuan Chen

Received: 31 March 2009 / Accepted: 5 June 2009 / Published online: 9 July 2009

Abstract A BET thermodynamic model and its recently modified version were applied to predict the phase diagrams of the systems NH_4NO_3–$LiNO_3$–H_2O and $NaNO_3$–$LiNO_3$–$Mg(NO_3)_2$–H_2O, in which two eutectic points were found with melting point at temperatures between 15 °C and 25 °C. Simple experiments were designed to measure the exothermal and endothermal behavior of the predicted phase change materials. The experimental results showed that the theoretically predicted materials possess excellent exothermal and endothermal behavior at room temperatures. Besides, the fusion and solidification heats of the predicted phase change materials were measured.

Keywords BET model · Phase change material · Hydrated salt · Phase diagram

Introduction

Energy shortage in the world makes it necessary to develop new energy resources, besides the traditional energy resources as fossil energy, water potential energy, wind energy and nuclear energy and so on. Direct adsorption and utilization of the environment-friendly and unexhausted sunshine has attracted more and more attentions. Phase change materials (PCM) have been proved to be an effect agent to carry out the direct utilization of the low grade energy. The utilization principle is described as follows: in the daytime when the sun is shine, the PCM adsorbs the sun energy by melting, and in night when the temperature decreases, the PCM releases a large amount of heat by crystallization. The materials are especially meaningful in the area, where the day-(or week-) temperature difference is large. To adsorb the sun energy and to release heat when the environmental temperature is slightly higher than and lower than room temperature, a PCM must meet many requirements, such as the cheap price, the light supercooled behavior, the weak corrosion, low toxicity, high heat capacity and stable behavior of charge and recharge of heat. Among them, the most important is that the material must melt and crystallize in the room temperature range of 15–25 °C. At best, the PCM melts and crystallizes at a stable temperature, so that it can adsorb and release the largest amount of heat in case the environmental temperature changes a little, and keep constant the environmental temperature.

Among all PCM, hydrated salts are found to have the largest latent heat capacity at temperatures below 423 K [1]. However, few hydrated salts with melting point at room temperatures are found up to now [1, 2]. Theoretically, when two or more hydrated salts are mixed, new eutectic materials may exist with melting point at room temperatures. To find the phase change materials in room temperatures, experimental methods are usually used [3–5]. While experiments are time and money consuming, theoretical prediction of phase diagram of prospective systems may be an effective approach. The prerequisite for a successful prediction of phase diagram is that the used theoretical model should possess a strong ability of prediction. For the salts used as possible PCMs are usually highly soluble, the prediction of properties for such highly soluble systems is a challenge for most thermodynamic models. In our previous works, BET thermodynamic model [6, 7] has been proved to be successful in the prediction of phase diagrams of highly soluble systems [8, 9]. When the

B. Li · D. Zeng (✉) · X. Yin · Q. Chen
College of Chemistry and Chemical Engineering, Central South University, Changsha 410083, People's Republic of China
e-mail: dewen_zeng@hotmail.com

salt–salt interactions in a predicted system are unnegligible, a modified BET model was proved to be more suitable [10–12].

In this paper, the phase diagrams of two prospective multi-component systems, NH_4NO_3–$LiNO_3$–H_2O and $NaNO_3$–$LiNO_3$–$Mg(NO_3)_2$–H_2O, are thermodynamically predicted. Of the predicted results two eutectic compositions with melting points at room temperatures are found. Further experiments related to the predicted PCM at room temperatures are carried out.

Modeling methodology

The BET model was first adapted by Stokes and Robinson [6] to describe the relation of water activity a_w and salt concentration m_s of a single salt–water system:

$$a_w m_s/(1-a_w) = 1/cr + ((1-c)/cr)a_w \quad (1)$$

where c and r are model parameters and can be obtained by fitting to experimental data of water activity.

For a multi-component system, Ally and Braunstein [7] have derived the BET model again on the basis of a statistical mechanical treatment of a multi-layer adsorption and given the expressions of component activity as follows:

$$a_w = \left(N_w - \sum_i N_{i(M)}\right)/N_w \quad (2)$$

$$a_i = \left(N_i/\sum_i N_i\right)\left\{\left(r_i N_i - N_{i(M)}\right)/(r_i N_i)\right\}^{r_i} \quad (3)$$

where a_w and a_i denote the activity of water and the salt i; N_w and N_i the mole number of water and the salt i; $N_{i(M)}$ the mole number of water bound to the salt i; r_i a BET parameter of the salt i, the same meaning as r in Eq. 1. The parameter values $N_{i(M)}$ are determined by solving the Eqs. 4, when the binary parameters r_i and c_i are known.

$$\frac{N_{i(M)}\sum_i N_{i(M)}}{(r_i N_i - N_{i(M)})(N_w - \sum_i N_{i(M)})} = c_i = \exp(-\Delta E_i/(RT)) \quad (4)$$

where c_i are the BET model parameters, $c_i = \exp(-\Delta E_i/RT)$, $\Delta E_i = (U_i - U_L)$, U_i is the energy of mono-layer adsorption of water onto the solute i, and U_L is the internal energy of liquefaction of pure water; R, general gas constant; T, thermodynamic temperature in Kelvin.

Considering the extra salt–salt interactions in the system as a regular solution [10–12], the Eq. 3 becomes:

$$a_i = \left(N_i/\sum_i N_i\right)\left\{\left(r_i N_i - N_{i(M)}\right)/(r_i N_i)\right\}^{r_i}\prod_{j\neq i}\exp\left(\frac{\Omega_{ij}}{RT}x_j\right) \quad (5)$$

where Ω_{ij} denotes an empirical interaction parameter between salt A and B, x_i the mole fraction of salt i in the anhydrous mixture.

Determination of model parameters

The binary BET parameters r_i and ΔE_i for the binary systems $NaNO_3$–H_2O, $LiNO_3$–H_2O, NH_4NO_3–H_2O and $Mg(NO_3)_2$–H_2O are taken from literatures [9, 11, 13] and listed in Table 1.

The chemical potential of formation of the solid salt·nH_2O $G^0_{Salt\cdot nH_2O}$, referring to pure hypothetic molten salts and pure water, as a function of temperature is obtained by calculating the activities of salt and water at binary liquidus points according to Eq. 6, when the BET parameters r_i and c_i (or ΔE_i) are known.

$$\begin{aligned} Salt\cdot nH_2O_{(s)} &= Salt_{(aq)} + nH_2O_{(aq)} \\ G^0_{Salt\cdot nH_2O} &= G_{Salt} + nG_{H_2O} \\ &= G^0_{Salt} + RT\ln a_{Salt} + nG^0_{H_2O} + nRT\ln a_w \\ &= RT\ln(a_{Salt}a_w^n) = RT\ln k_{Salt\cdot nH_2O} \end{aligned} \quad (6)$$

where the values of G^0_{Salt} and $G^0_{H_2O}$ are set to be zero at any temperature. The parameters $G^0_{Salt\cdot nH_2O}$, obtained in this way are tabulated in Table 2.

Figure 1 is the phase diagram of the system NH_4NO_3–$LiNO_3$–H_2O calculated by the parameters in Table 1 and 2. When the contents of NH_4NO_3 and $LiNO_3$ are competitable, considerable differences arise between the predicted and experimental [16] isotherms reported by Campbell in 1942. It should be mentioned that even in the binary system $LiNO_3$–H_2O, our calculated saturation points for solid phase $LiNO_3$(s) are different from the experimental ones [16]. However, our model parameters for the system $LiNO_3$–H_2O are elaborately prepared and the calculated binary liquidus agrees with our experimental data [11] quite well, as well as that given by Campbell and Bailey [17] in 1958. Fitting the parameter $\Omega_{i,j}$ for NH_4NO_3 and $LiNO_3$ in Eq. 5 to the experimental solubility [16], one obtains the parameter value $\Omega_{i,j} = 2759.3 - 14.286T$ J mol^{-1}, with which the ternary phase diagram is simulated again and the result is shown in Fig. 2.

Table 1 Binary BET parameters

Salt	r*		ΔE**		Source
	a	b	c	d	
$NaNO_3$	1.8	0	−1000	0	[9]
$LiNO_3$	2.766	0.000143	−6583.6	5.495	[11]
NH_4NO_3	1.63	0	890	0	[13]
$Mg(NO_3)_2$	5.579	0	0	−31.348	[9]

* r = a + b(T/K); ** ΔE/(J mol^{-1}) = c + d(T/K)

Table 2 Temperature coefficients of chemical potential of the solid salt·nH_2O $G^0_{Salt\cdot nH_2O}$*

Solid phase	Parameters			Temperature range, T/K	Solubility data for parameter determination
	A	B	C		
$LiNO_3\cdot 3H_3O$	11057.869	−1235.211	198.82931	273–301	[11]
$LiNO_3$	−4963.150	−209.61589	35.05814	303–333	[11]
$NaNO_3$	−15699.33	26.9207	0	273–292	[14]
NH_4NO_3	29822.983	436.06597	−60.704671	293–368	[15]
$Mg(NO_3)_2\cdot 6H_2O$	−29342.6	−115.008	0	373–428	[15]
$Mg(NO_3)_2\cdot 2H_2O$	−20297.8	−42.8	0	328–400	[15]

* $G^0_{Salt\cdot nH_2O}/(J\ mol^{-1}) = RT\ln k_{Salt\cdot nH_2O} = A+B(T/K) + CT\ln(T/K)$

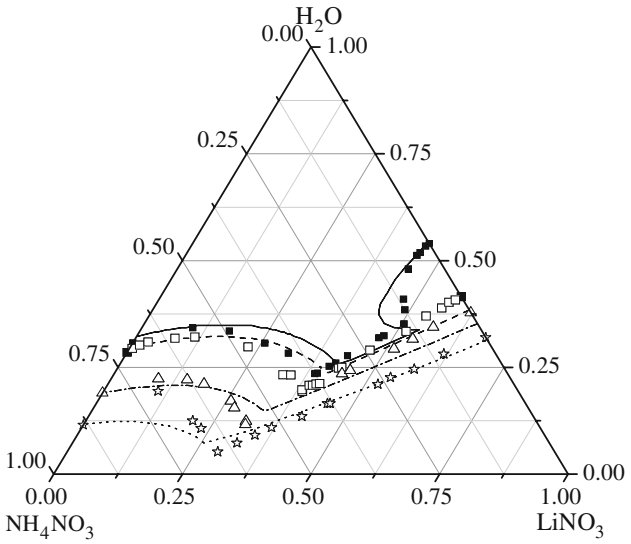

Fig. 1 Predicted isotherms comparing with the experimental data in the system NH_4NO_3–$LiNO_3$–H_2O. *Lines*: Predicted, ——: 298.15 K, – – –: 304.15 K, –·–: 333.15 K, ····: 363.15 K. *Symbols*: Exp. [16], ■: 298.15 K, □: 304.15 K, △: 333.15 K, ☆: 363.15 K

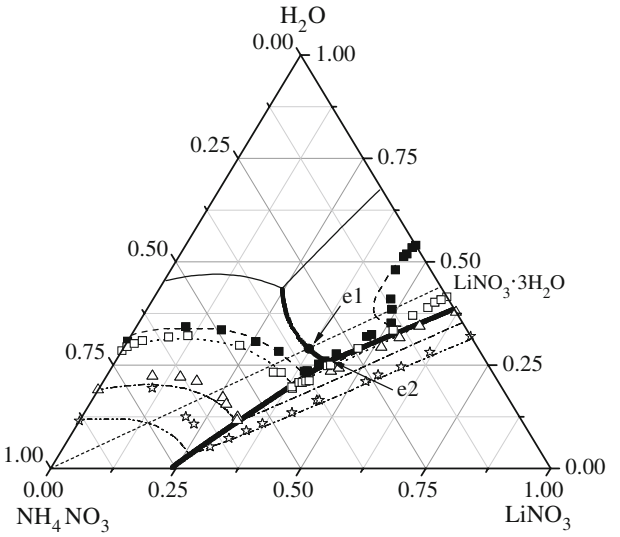

Fig. 2 Solubility phase diagram of the system NH_4NO_3–$LiNO_3$–H_2O. *Lines*: Isotherm predicted, —— (thin): 273.15 K, — —: 298.15 K, ·····: 304.15 K, –·–: 333.15 K, –··–: 363.15 K, – –: Cross section line, □ (wide): Univariant line. *Symbols*: Exp.[16], ■: 298.15 K, □: 304.15 K, △: 333.15 K, ☆: 363.15 K, ●: Predicted eutectic points

Predicted solubility phase diagrams and phase change materials

In Fig. 2 two eutectic points are predicted, the qua-binary eutectic point NH_4NO_3–$LiNO_3\cdot 3H_2O$ and the ternary eutectic point NH_4NO_3–$LiNO_3$–$LiNO_3\cdot 3H_2O$, whose melting temperatures fall near 16 °C. The compositions of the eutectic points are listed in Table 3.

In the previous papers [9], the solubility diagrams of the systems $NaNO_3$–$LiNO_3$–H_2O and $LiNO_3$–$Mg(NO_3)_2$–H_2O have been predicted in the BET model. After we elaborately measured the solubility of the system $LiNO_3$–H_2O, more accurate model parameters for this system have been obtained [11]. In this case, the solubility diagram of the ternary systems $NaNO_3$–$LiNO_3$–H_2O and $LiNO_3$–$Mg(NO_3)_2$–H_2O are predicted again. The predicted results compared with experimental data [18–20] are presented in Figs. 3 and 4. Good agreements have been found between the predicted and experimental ones. In the two ternary systems four eutectic points have been predicted with melting temperature slightly higher than room temperature, as shown in Table 3. This stimulates our curiosity and we strongly expect to know if the combination of the phases $NaNO_3$, $LiNO_3\cdot 3H_2O$ and $Mg(NO_3)_2\cdot 6H_2O$ will form a quaternary eutectic point with melting temperature in the room temperature range. To this purpose, the solubility phase diagram of the system $NaNO_3$–$LiNO_3$–$Mg(NO_3)_2$–H_2O is partly predicted and the predicted diagram is shown in Fig. 5, where, one can see that a quaternary eutectic point exists with melting temperature at 297.4 K, of which the composition is listed in Table 3.

Table 3 Predicted eutectic points with melting temperatures and compositions

Eutectic points	*T*/K	Composition/100 w
NH_4NO_3–$LiNO_3{\cdot}3H_2O$	289.1	$LiNO_3{\cdot}3H_2O$:66.17, NH_4NO_3:33.83
NH_4NO_3–$LiNO_3$–$LiNO_3{\cdot}3H_2O$	287.72	$LiNO_3$:42.30, NH_4NO_3:32.0, H_2O:25.70
$NaNO_3$–$LiNO_3{\cdot}3H_2O$	300.8	$LiNO_3{\cdot}3H_2O$:92.1, $NaNO_3$:7.9
$NaNO_3$–$LiNO_3$–$LiNO_3{\cdot}3H_2O$	299.21	$LiNO_3$:57.0, $NaNO_3$:6.6, H_2O:36.40
$LiNO_3{\cdot}3H_2O$–$Mg(NO_3)_2{\cdot}6H_2O$	299.3	$LiNO_3{\cdot}3H_2O$:70.8, $Mg(NO_3)_2{\cdot}6H_2O$:29.2
$LiNO_3{\cdot}3H_2O$–$LiNO_3$–$Mg(NO_3)_2{\cdot}6H_2O$	299.66	$LiNO_3$:47.5, $Mg(NO_3)_2$:13.0, H_2O:39.5
$LiNO_3{\cdot}3H_2O$–$Mg(NO_3)_2{\cdot}6H_2O$–$NaNO_3$	297.4	$LiNO_3{\cdot}3H_2O$:67.4,$Mg(NO_3)_2{\cdot}6H_2O$:26.9, $NaNO_3$:5.7

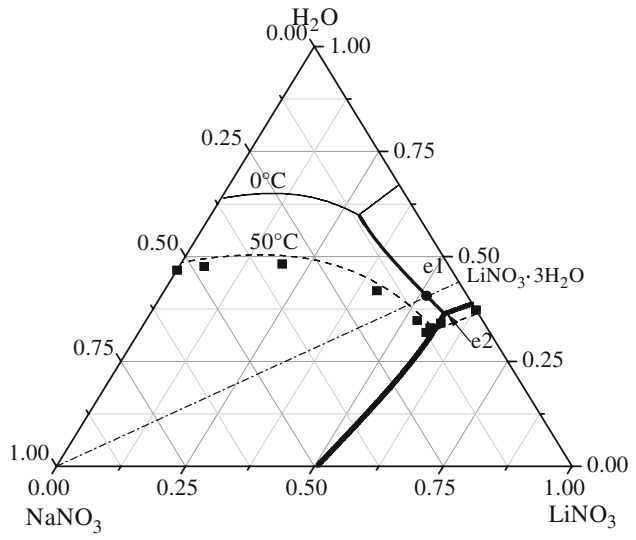

Fig. 3 Predicted solubility phase diagram of the system $NaNO_3$–$LiNO_3$–H_2O and its comparison with experimental data. *Lines*: Predicted, —— (thin): 273.15 K, – – –: 323.15 K, –·–: Cross section line, —— (thick): Univariant line. *Symbols*: Exp. [18], ■: 323.15 K, ●: Predicted eutectic points

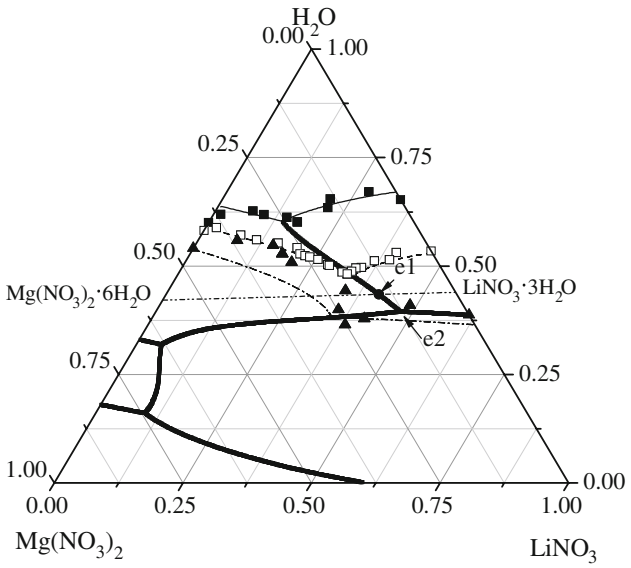

Fig. 4 Predicted solubility phase diagram of the system $Mg(NO_3)_2$–$LiNO_3$–H_2O and its comparison with experimental data. *Lines*: Isotherm predicted, —— (thin): 273.15 K, – – –: 298.15 K, –·–: 323.15 K, –···–: Cross section line, —— (thick): Univariant line. Symbols: Exp, ■: 273.15 K [19], □: 298.15 K [20], ▲: 323.15 K [19], ●: Predicted eutectic points

Experimental

To measure the melting and crystallization behavior of the predicted materials in Table 3, a device shown in Fig. 6 was designed. A two liter beaker was placed in a water bath whose temperature, as environmental temperature, was kept at a constant value by a temperature controller and recorded by a computer. A tube of 100 ml containing 50 games phase change materials was fixed in the center of the beaker. A temperature sensor of copper was immersed in the center of the phase change material and the temperature change was recorded by the computer.

On each measurement the temperature of the water bath was controlled at a certain value at first, and then the tube containing the 50 games phase change material was moved into the beaker and the temperature in the phase change material was recorded in the computer.

Differential scanning calorimeter (DSC Q10, TA Instruments) was used to measure the fusion temperature T_f, fusion heat H_f, solidification temperature T_s and heat of solidification H_s of the two predicted PCMs at room temperatures. At first, the two predicted PCMs were placed at −10 °C until all were solidified completely; then, some 10 mg samples were taken into the sample pan with cover; the temperature was raised to 40 °C at a rate of 10 °C min^{-1}. On reaching 40 °C, the temperature was controlled to drop to −10 °C again at the same rate. To test the stability of the PCMs, this cycle was repeated three times.

All the chemical reagents: NH_4NO_3, $Mg(NO_3)_2$, $LiNO_3$ and $NaNO_3$ for the preparation of the phase change materials are of analytical purity.

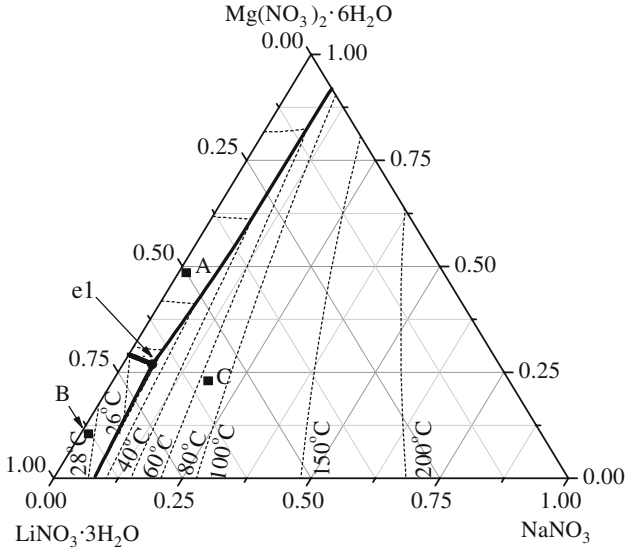

Fig. 5 Predicted solubility phase diagram of the quaternary system $NaNO_3$–$LiNO_3{\cdot}3H_2O$–$Mg(NO_3)_2{\cdot}6H_2O$. – – –: Isotherms, —— (thick): Univariant line, ●: Predicted eutectic point

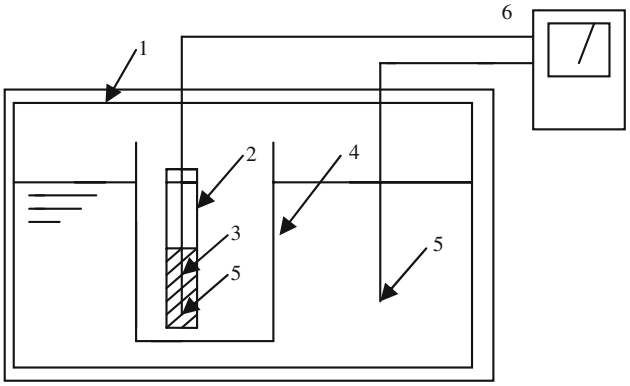

Fig. 6 Schematic device for measuring the phase change material. (1) water bath, (2) test tube with plug, (3) phase change material, (4) glass beaker, (5) temperature sensor of copper, (6) temperature recorder

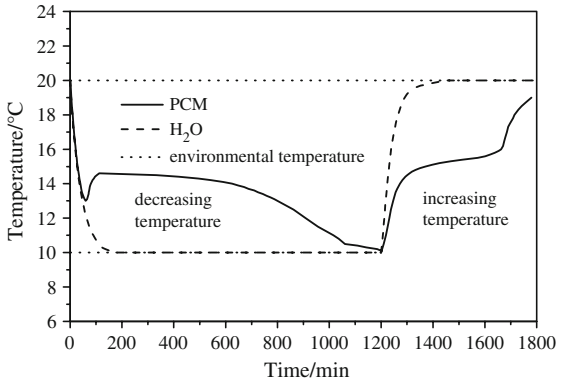

Fig. 7 Temperature curve of PCM (*e1* in Fig. 2) and water as a function of time

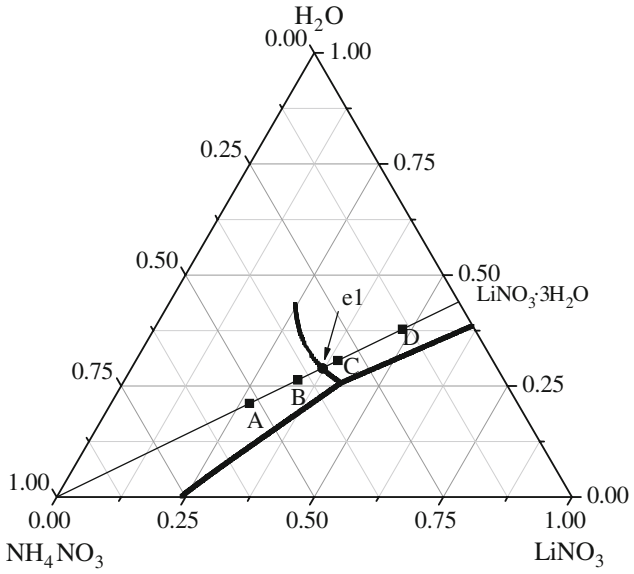

Fig. 8 Schematic composition map of the system $LiNO_3{\cdot}3H_2O$–NH_4NO_3 for experimental measurement. *Lines*: —— (wide): Univariant line, —— (thin): Cross section line. *Symbols*: *e1* Predicted eutectic composition, A, B C, D: compositions for comparison

Results and discussion

System $LiNO_3NH_4NO_3$–H_2O

The measured temperature change of the predicted PCM (point e1 in Fig. 2) in different environmental temperatures (20 °C or 10 °C) is shown in Fig. 7. The average measured phase change temperature is about 15 °C, one Celsius lower than the predicted one. Besides, the exothermal and endothermal behaviors of PCMs at compositions other than the predicted point e1, as schematically shown with A, B, C and D in Fig. 8 are measured and presented in Fig. 9. It can be seen that when the content of NH_4NO_3 is more than needed for the eutectic point e1, as illustrated in point A and B in Fig. 8, the temperature platforms (see Fig. 9a, b) keep in shorter time than that of the predicted eutectic point e1 (see Fig. 7). It is reasonable that the heat storage ability decreases when some NH_4NO_3 in the PCM does not melt. When the content of $LiNO_3{\cdot}3H_3O$ is more than needed for the eutectic point e1, as illustrated in points C and D in Fig. 8, the temperature platforms (Fig. 9c, d) do not keep any more, especially in the process of increasing temperature.

System $LiNO_3$–$NaNO_3$–H_2O

In the system $LiNO_3$–$NaNO_3$–H_2O two eutectic points (e1 and e2 in Fig. 3) are predicted with melting point at about 27 °C. Since the PCM at e1 contains less amount of

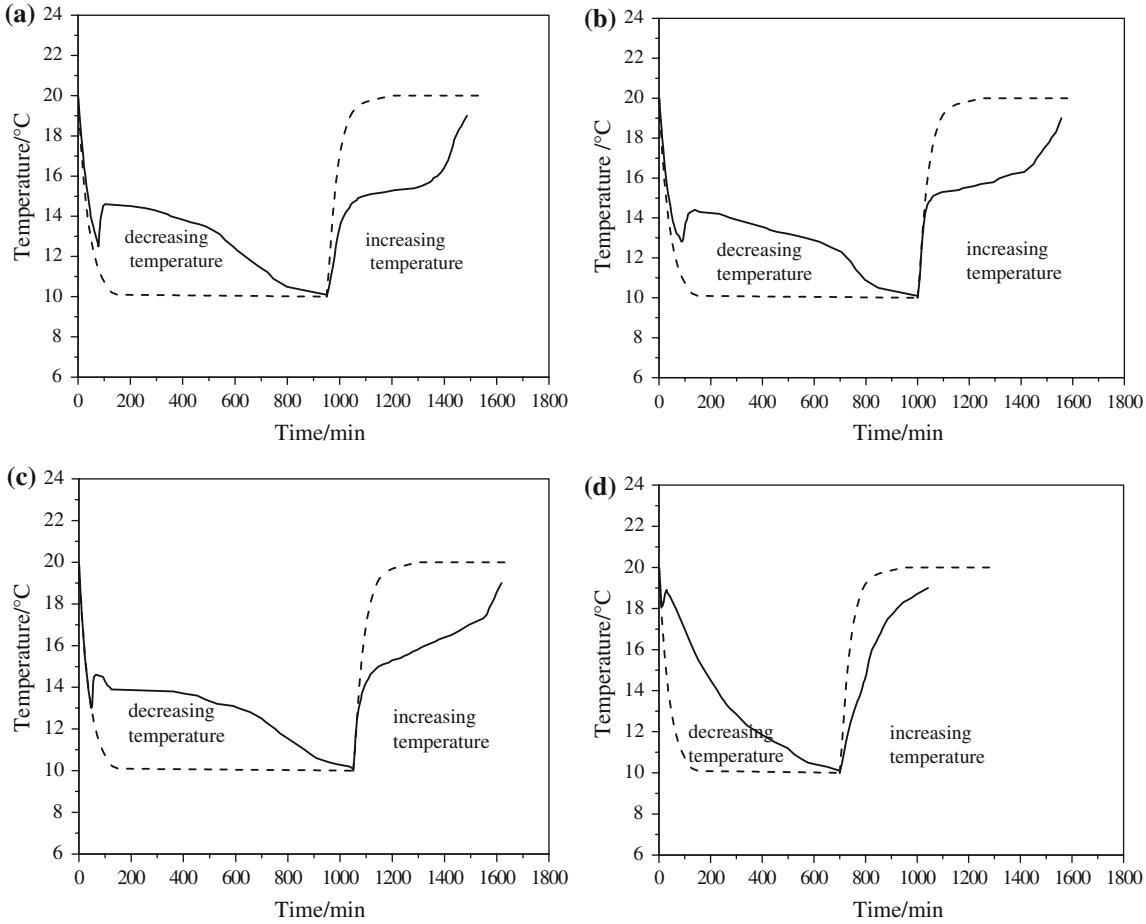

Fig. 9 Temperature change curve of PCMs (A, B, C and D in Fig. 8) and water. ——: PCM, – – –: water

expensive $LiNO_3$ than that at e2 and their melting temperatures are similar, the composition e1 can be more economical and thus its heat storage behavior is checked experimentally. The measured result is shown in Fig. 10. It can be seen that the measured phase change temperature is about 27 °C and identical to the predicted one in Fig. 3.

System $LiNO_3$–$Mg(NO_3)_2$–H_2O

The eutectic point e1 predicted in Fig. 4 consisting of $Mg(NO_3)_2{\cdot}6H_3O$ and $LiNO_3{\cdot}3H_3O$ is checked experimentally and the result is presented in Fig. 11. The experimental phase change temperature lies between 25 °C and 26 °C, comparing to the theoretically predicted temperature of 26.1 °C.

System $LiNO_3$–$NaNO_3$–$Mg(NO_3)_2$–H_2O

The heat storage behavior of the predicted eutectic point e1 in Fig. 5 is measured and presented in Fig. 12(e1). The measured melting temperature of the PCM falls in the temperature range of 23.8 and 24.8 °C, quite near the

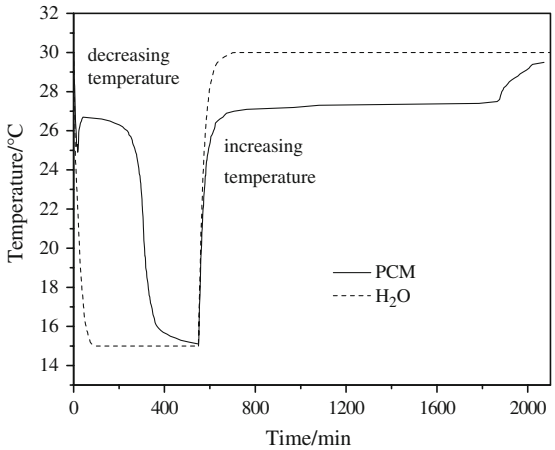

Fig. 10 Temperature curve of PCM (*e1* in Fig. 3) and water

predicted phase change temperature of 24.3 °C. One can say that the theoretically predicted eutectic composition and temperature in the quaternary system $NaNO_3$–$LiNO_3{\cdot}3H_3O$–$Mg(NO_3)_2{\cdot}6H_2O$ is quite reliable. Meanwhile, the PCMs at compositions other than the predicted point e1, as shown in points A, B and C in Fig. 5, are also

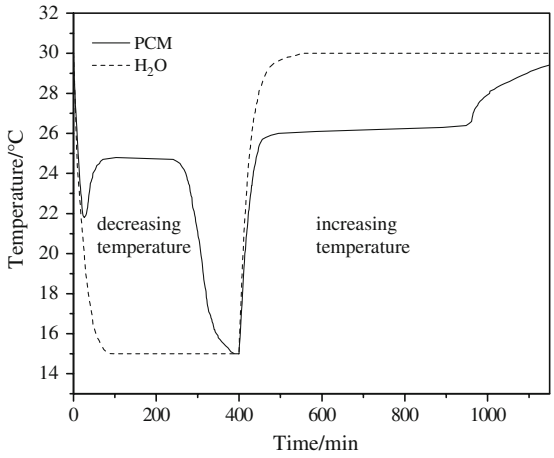

Fig. 11 Temperature curve of PCM (*e1* in Fig. 4) and water as a function of time

measured and presented in Figs. 12a, b and c. For the compositions A and B in Fig. 5, no platform exists both on the process of increasing and decreasing temperature (see Fig. 12a, b). When the content of $NaNO_3$ is more than the predicted point, for example, point C in Fig. 5, although two temperature platforms form, but obviously keep in shorter time than that of the predicted eutectic (see Fig. 12a).

DSC measurement of the PCMs

The DSC result of the PCM (point e1 in Fig. 2) is presented in Fig. 13. In the three cycles, the measured fusion temperature T_f is 16.01 °C, 16.01 °C, 16.00 °C and fusion heat H_f are 187.1 J g^{-1}, 187.1 J g^{-1}, 186.95 J g^{-1} respectively. However, the solidification temperature T_s is 14.98 °C, 14.98 °C, 14.97 °C and the solidification heat H_s is 175.9 J g^{-1}, 175.9 J g^{-1}, 175.8 J g^{-1}, respectively. The difference between that of melting and solidifying is reasonable, considering the difference of temperature between the sample and environment. The average phase change temperature is 15.5 °C, 0.5 °C lower than the predicted one. The average phase change heat is 181 J g^{-1}.

The DSC result of the PCM (point e1 in Fig. 5) is presented in Fig. 14. In the three cycles, the measured fusion temperature T_f is 24.78 °C, 24.78 °C, 24.77 °C and solidification temperature 23.65 °C, 23.65 °C, 23.64 °C, respectively. The average phase change temperature is 24.2 °C, 0.2 °C lower than the predicted one (see Table 3). The fusion heat H_f is 169.1 J g^{-1}, 169.1 J g^{-1}, 168.9 J g^{-1} and solidification heat H_s 158.9 J g^{-1}, 158.9 J g^{-1}, 158.8 J g^{-1}, respectively. The average phase change heat is 165 J g^{-1}.

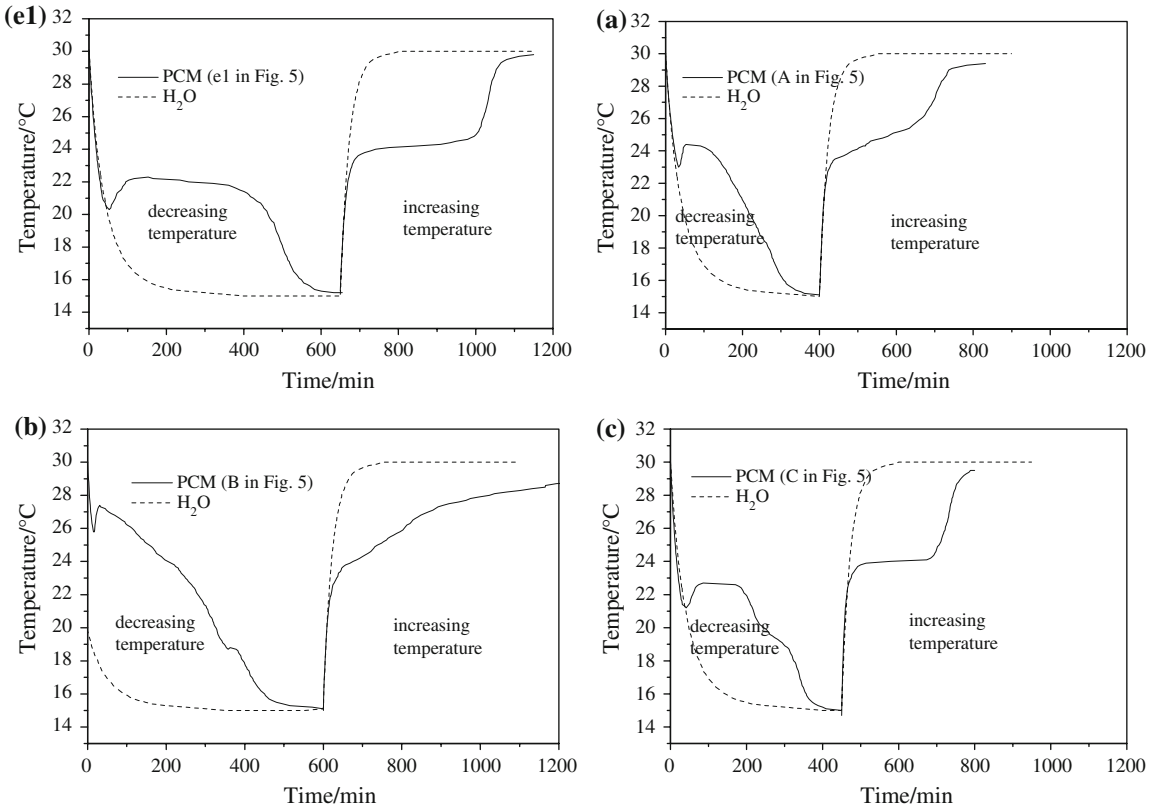

Fig. 12 Temperature curve of PCM (*e1*, A, B, C in Fig. 5) and water as a function of time

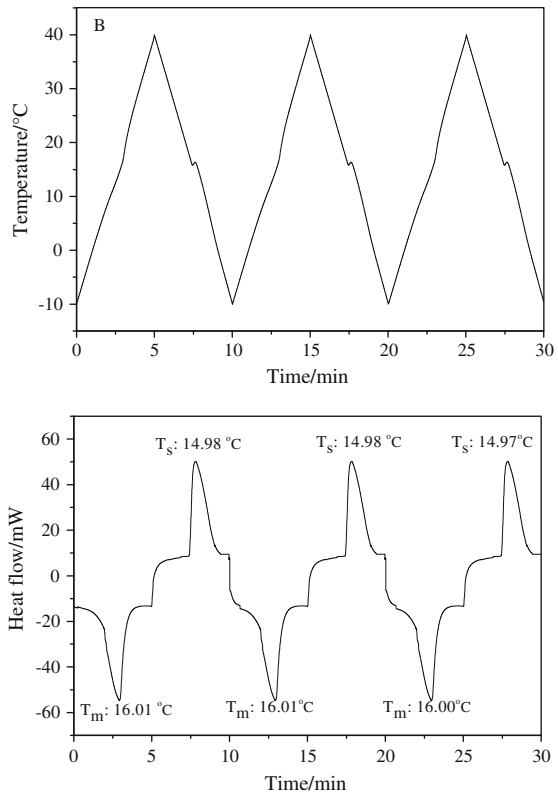

Fig. 13 DSC of the PCM (*e1* in Fig. 2)

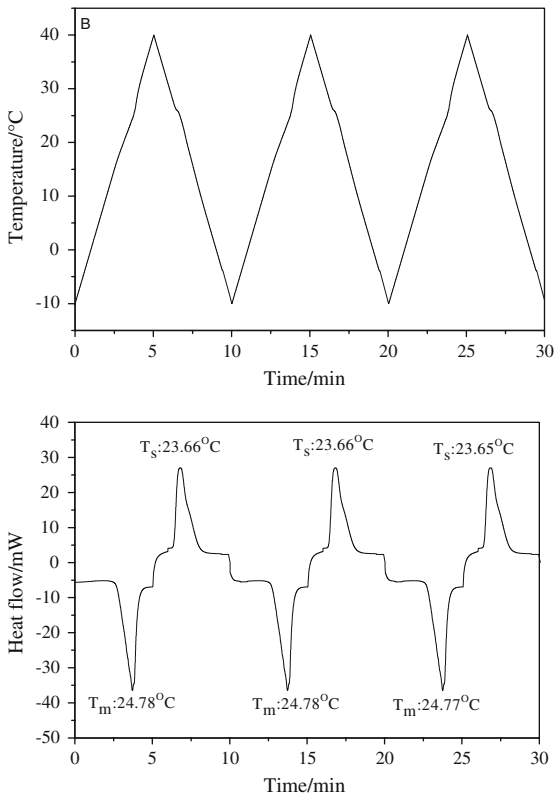

Fig. 14 DSC of the PCM (*e1* in Fig. 5)

Conclusions

In this paper we applied the modified BET model to describe and predict the solubility phase diagrams of the binary systems NH_4NO_3–H_2O, $LiNO_3$–H_2O, $NaNO_3$–H_2O, $Mg(NO_3)_2$–H_2O and the ternary system NH_4NO_3–$LiNO_3$–H_2O, $LiNO_3$–$NaNO_3$–H_2O, $NaNO_3$–$Mg(NO_3)_2$–H_2O, $LiNO_3$–$Mg(NO_3)_2$–H_2O and the quaternary system $LiNO_3$–$NaNO_3$–$Mg(NO_3)_2$–H_2O, finding two eutectic points with melting temperature at room temperatures in the systems NH_4NO_3–$LiNO_3{\cdot}3H_2O$ and $NaNO_3$–$LiNO_3{\cdot}3H_2O$–$Mg(NO_3)_2{\cdot}6H_2O$. And then, a device was designed to measure the heat storage behavior of the predicted room temperature PCMs, as well as some non-predicted PCMs in these systems. Besides, the theoretically predicted PCMs were measured by DSC in three cycles. It was found that the phase change temperature and heat of the theoretical composition (66.17 wt% $LiNO_3{\cdot}3H_2O$, 33.83 wt% NH_4NO_3) are 15.5 °C and 181 J g^{-1}, respectively; the phase change temperature and heat of the theoretical composition (67.4 wt% $LiNO_3{\cdot}3H_2O$, 26.9 wt% $Mg(NO_3)_2{\cdot}6H_2O$, 5.7 wt% $NaNO_3$) are 15.5 °C and 181 J g^{-1}, respectively. Both predicted PCMs possess excellent thermal stability and reversibility.

By comparing the heat storage behavior of the theoretically predicted and non-predicted PCMs, one can see what roles a thermodynamic model can play in the design of room temperature PCMs consisting of hydrated salts.

Acknowledgements This work is financially supported by the Ministry of Science and Technology, PR China, under contract number 2006AA05Z212 and 2006CB708640.

References

1. Hasnain SM. Review on sustainable thermal energy storage technologies part I: heat storage materials and techniques. Energy Convers Manage. 1998;39:1127–38.
2. Voigt W, Zeng D. Solid-liquid equilibria in mixtures of molten salt hyrates for the design of heat storage materials. Pure Appl Chem. 2002;74:1909–20.
3. Nagano K, Mochida T, Takeda S, Domanski R, Rebow M. Thermal characteristics of manganese (II) nitrate hexahydrate as a phase change material for cooling system. Appl Therm Eng. 2003;23:229–41.
4. Nagano K, Ogawa K, Mochida T, Hayashi K, Ogoshi H. Thermal characteristics of magnesium nitrate hexahydrate and magnesium chloride hexahydrate mixture as a phase change material for effective utilization of urban waste heat. Appl Therm Eng. 2004;24:209–20.
5. Nagano K, Ogawa K, Mochida T, Hayashi K, Ogoshi H. Performance of heat charge/discharge of magnesium nitrate hexahydrate and magnesium chloride hexahydrate mixture to a single vertical tube for a latent heat storage system. Appl Therm Eng. 2004;24:221–32.
6. Stokes RH, Robinson RA. Ionic hydration and activity in electrolyte solutions. J Amer Chem Soc. 1948;70:1870–8.

7. Ally MR, Braunstein J. Statistical mechanics of multilayer adsorption: electrolyte and water activities in concentrated solutions. J Chem Thermodyn. 1998;30:49–58.
8. Voigt W. Calculation of salt activities in molten salt hydrates applying the modified BET equation (I): binary system. Monatsh Chem. 1993;124:839–48.
9. Zeng D, Voigt W. Phase diagram calculation of molten hydrates using the modified BET equation. Calphad. 2003;27:243–51.
10. Zeng D, Liu H, Chen Q. Simulation and prediction of solubility phase diagram for the separation of $MgCl_2$ from LiCl brine using HCl as a salting-out agent. Hydrometallurgy. 2007;89:21–31.
11. Zeng D, Ming J, Voigt W. Thermodynamic study of the system LiCl–$LiNO_3$–H_2O. J Chem Thermodyn. 2008;40:232–9.
12. Zeng D, Xu W, Voigt W, Yin X. Thermodynamic study of the system LiCl–$CaCl_2$–H_2O. J Chem Thermodyn. 2008;41:1157–65.
13. Rains WO, Cownce RM. Liquidus curves of NH_4NO_3(aq) calculated from the modified adsorption isotherm model for aqueous electrolytes. Sep Sci Technol. 2006;41:2629–34.
14. Ally MR. Liquidus curve of $NaNO_3$(aq) calculated from the modified adsorption isotherm model for aqueous electrolytes. Monatsh Chem. 2000;131:341–4.
15. Linke WF, Seidell A. Solubilities of inorganic and metal organic compounds. 4th ed. Washington: American Chemical Society; 1965. p. II423. (p. II511, p. II709).
16. Campbell AN. The system: $LiNO_3$–NH_4NO_3 and $LiNO_3$–NH_4NO_3–H_2O. J Amer Chem Soc. 1942;64:2680–4.
17. Campbell AN, Bailey RA. The system lithium nitrate–ethanol–water and its component binary systems. Can J Chem. 1958; 36:518–36.
18. Andronova NP. Solium nitrate–lithium nitrate–water system at 50 deg. Uch Zap Yarosl Gos Ped Inst. 1972;103:50–1.
19. Chernykh LV, Bulgakova TN, Skripkin MYu. Thermodynamic study of MgX_2–LiX–H_2O system (X = Br, NO_3, ClO_4) at 0 and 50 °C. Zh Prikl Khim. 1998;71:1425–30.
20. Zbranek V, Eysseltova J. Study of the ternary systems M(II) $(NO_3)_2$–$LiNO_3$–H_2O (M(II) = Mg, Ca, Sr, Ba) at 25 °C. Monatsh Chem. 2001;132:1463–75.